Tetramethylpiperidine–Alane Adducts tmpH · AlX_3 (X = Cl, Br, I) and tmpH · AlH_2Cl: Synthesis, Solution Behavior, and X-ray Crystal Structures☆

Ingo Krossing[1], Heinrich Nöth*, Holger Schwenk-Kircher[2], Thomas Seifert[2], and Christiane Tacke

Institut für Anorganische Chemie der Universität München,
Meiserstraße 1, D-80333 München, Germany
Fax: (internat.) + 49(0)89/5902451

Received November 27, 1997 (Revised September 2, 1998)

Keywords: Tetramethylpiperidine–aluminum trihalide adducts / Tetramethylpiperidine–monochloroalane / Conductivity measurements / ^{27}Al-NMR spectroscopy

2,2,6,6-Tetramethylpiperidine (tmpH) reacts smoothly with aluminum trihalides AlX_3 (X = Cl, Br, I) and monochloroalane $AlH_2Cl \cdot 2$ thf to give the addition compounds tmpH · AlX_3 (X = Cl, Br, I) and tmpH · AlH_2Cl, respectively. These adducts of the secondary amine tmpH are stable and do not undergo intramolecular elimination of HX or H_2 with formation of the aminoalanes $tmpAlX_2$ or tmpAl(H)Cl. In the solid state, tmpH · AlX_3 (X = Cl, Br, I) and tmpH · AlH_2Cl are tetracoordinated molecular adducts. While this is also true for solutions of tmpH · AlX_3 (X = Br, I) and tmpH · AlH_2Cl, the compound tmpH · $AlCl_3$ dissolves in CH_2Cl_2 as the salt $[tmpAlCl_3]$-$tmpH_2$ and the adduct tmpH · Al_2Cl_6, as is evident from its NMR spectra and from conductivity measurements. This behavior is supported by a semiempirical AM1 calculation.

Due to their importance in industrial processes, addition compounds of aluminum halides AlX_3 (in particular X = Cl) and ether donors have been the subject of extensive studies with regard to their solution and solid-state behavior[3]. Depending on the method of preparation, the tetra-, penta-, or hexacoordinated species $AlX_3 \cdot Do_n$ (Do = ether donor; $n = 1-3$) exist either as molecular adducts[4][5] or as salts {e.g. $AlCl_3 \cdot (thf)_2$ and $[AlCl_2(thf)_4]AlCl_4$}. The latter is also true for the addition compounds with pyridine[6], DMSO[7], and acetonitrile[8] (L), leading to the general compound type $[AlCl_2L_4^+]$-AlX_4^-. In solution, salt formation can readily be detected by ^{27}Al-NMR and conductivity measurements, including Fuoss-Kraus plots for analysis of the dissociation patterns[9]. Owing to facile H_2 or HX elimination, the chemistry of the addition compounds of the aluminum halides AlX_3 or AlH_2X (X = Cl, Br, I) with primary or secondary amines has scarcely been examined. However, two recent publications demonstrate the existence and importance of these species: Raston et al.[10] described a stable AlH_3 adduct with the sterically encumbered secondary amine tmpH (2,2,6,6-tetramethylpiperidine), while Atwood[11] later observed salt formation upon the addition of excess *t*$BuNH_2$ to R_2AlX (X = Cl, Br, I; R = Me, Et) when chloride was replaced by bromide or iodide. Recently, we reported on the synthesis of monomeric bis(tetramethylpiperidino)aluminum halides tmp_2AlX (X = Cl, Br, I) and on their derivatives[12]. In the course of these studies, addition compounds of tmpH and AlX_3 (X = Cl, Br, I) and AlH_2Cl were identified as by-products. For their full characterization, these adducts tmpH · AlX_3 [X = Cl (**1a**), Br (**1b**), I (**1c**)] and tmpH · AlH_2Cl (**2**) have now been independently synthesized from their respective components. Herein, we report on their solution and solid-state behavior.

Synthesis and Characterization

Addition of one equivalent of tmpH to $AlCl_3$ (in CH_2Cl_2) or $AlBr_3$, AlI_3, and $AlH_2Cl \cdot 2$(thf) solutions (in toluene) leads to immediate formation of the adducts tmpH · AlX_3 [X = Cl (**1a**), Br (**1b**), I (**1c**)] and tmpH · AlH_2Cl (**2**).

$$tmpH + AlX_3 \longrightarrow tmpH^*AlX_3 \quad (1a)$$
X = Cl **1a**, Br **1b**, I **1c**

$$tmpH + AlH_2Cl^*thf_2 \longrightarrow tmpH^*AlH_2Cl + 2\,thf \quad (1b)$$
2

Evolution of hydrogen or HX was not observed. **1b**, **c** and **2** proved to be molecular monomers in benzene solution. They give rise to single sharp signals in the ^{27}Al-NMR spectra. The chemical shifts of these addition compounds follow the substitution pattern, the iodide being observed at highest field ($\delta^{27}Al = 12$, $\Delta_{1/2} = 140$ Hz), followed by the bromide ($\delta^{27}Al = 88$, $\Delta_{1/2} = 130$) and AlH_2Cl ($\delta^{27}Al = 123$). Distinct lines for axial and equatorial methyl groups (^{1}H- and ^{13}C-NMR) as well as for the ring-hydrogen atoms (^{1}H-NMR) are observed. Thus, axial and equatorial positions of the hydrogen and carbon atoms in the piperidine ring in **1b**, **c** are magnetically inequivalent.

Whereas **1b**, **c** and **2** retain their molecular character upon dissolution in aromatic and chlorinated solvents, the chloro compound **1a** behaves differently. In the solid state, **1a** exists as a tetracoordinated molecular adduct of the type tmpH · $AlCl_3$ (vide infra), but in solution it disproportionates according to Eq. 2.

Two signals at $\delta^{27}Al = 108$ and 106, $\Delta_{1/2} = 120$ and 47 Hz, with an integral ratio of 2:1 are found (100°C), corresponding to a conversion of **1a** to tmpH · Al_2Cl_6 and

  1434–1948/98/1212–1925 $ 17.50+.50/0

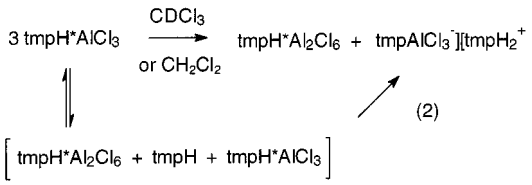

$[tmpAlCl_3]tmpH_2$. The line widths of the ^{27}Al-NMR signals are found to be temperature-dependent. At 0°C, only one broad line at $\delta^{27}Al = 106$ is observed. Heating the sample to 100°C ($[D_8]$toluene) leads to the resolution of two well-separated lines (see Figure 1), indicating the absence of rapid exchange processes and the presence of two distinct species.

Figure 1. ^{27}Al-NMR spectra of tmpH · $AlCl_3$ (**1a**) at various temperatures ($[D_8]$toluene)

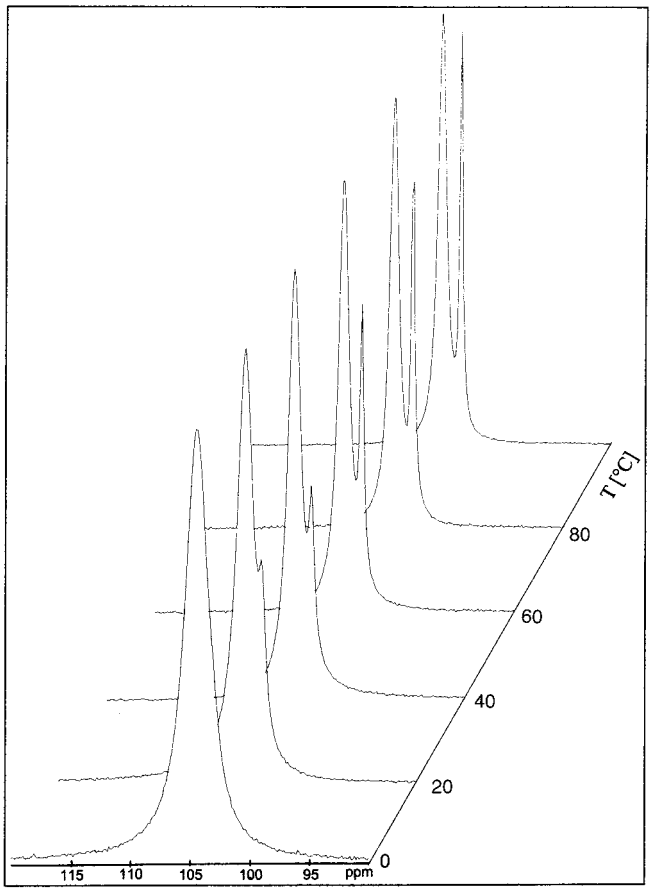

The "dissociation" of **1a** is indicated by the appearance of three sets of signals for the different tmp ligands, represented by the formulae (tmpH · Al_2Cl_6; $[tmpAlCl_3]tmpH_2$). Two signals are observed in the range $\delta = 57-60$ for the carbon atoms bonded to nitrogen atoms, indicating the presence of two distinct tmp groups with tetracoordinated nitrogen atoms. The third ligand has a tricoordinated nitrogen atom, since the respective ^{13}C(C−N) resonance is found at $\delta = 53.2$ {cf. for example tmpAlI_2 · py: $d^{13}C(C-N) = 53.3$ (tricoordinated nitrogen atom); $[(Me_3Si)_3SiAlCl_3]$ $tmpH_2$: $d^{13}C(C-N) = 58.0$ (tetracoordinated nitrogen atom)}[12][13]. Furthermore, two broad lines for the N−H protons in a ratio of 2:1 (1:6 and 1:12 to each of the tmp methyl signals) as well as three distinct tmp methyl groups are observed in the ^{1}H-NMR spectrum.

To further prove the "dissociation" pattern of the salt $[tmpAlCl_3]tmpH_2$ (as represented by Eq. 2), **1a** has been subjected to conductivity measurements in CH_2Cl_2.

Figure 2. Fuoss-Kraus plot for tmpH · $AlCl_3$ (**1a**) calculated from conductivity measurements in CH_2Cl_2

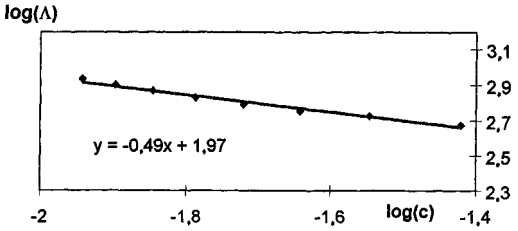

According to the gradient of the Fuoss-Kraus[14] plot ($a = -0.5$, depicted in Figure. 2), the solution contains a simple A^+B^- system. Since the molecular adduct tmpH · Al_2Cl_6 is not involved in ion formation, only the conductivity induced by the $[tmpAlCl_3]tmpH_2$ species, an A^+B^- compound, is detected.

Crystal Structures

In contrast to the solution behavior of **1a**, the structures of **1a** (Figure 3), **1b** (Figure 4), **1c** (Figure 5), and **2** (Figure 6) in the solid state all represent simple adducts with tetracoordinated aluminum centers. Crystals of **1a−c** are found to be monoclinic, space group $P2_1/n$ (**1a**) and $P2_1/c$ (**1b**, **c**), respectively, while **2** crystallizes in the orthorhombic space group $P2_12_12_1$. All unit cells contain four molecules. Selected structural parameters are summarized in Table 1.

In each of the adducts, the aluminum atom is coordinated by a nitrogen atom, with the halogen and/or hydrogen atoms arranged in a distorted tetrahedral manner. Whereas the angles X−Al−X in **1a−c** are close to 109.5°, the N−Al−X bond angles deviate by +9.7/−10.5° from this value. This behavior seems to depend on the size of the halogen atoms, as these deviations are reduced to +2.5 and −8.3°, respectively, in **2**. One halogen atom resides between the two equatorial methyl groups, on the same side as the N−H atoms. The respective H−N−Al−X torsion angles vary from 7.38° (**1a**), through 5.0° (**1b**) and 0.3° (**1c**), to 23.5° (**2**). The geometry at the nitrogen atom (C_2NAl plane) is close to planar, as is indicated by the sums of the respective bond angles (**1a**: 350.1°; **1b**: 350.2°; **1c**: 350.3°; **2**: 346.5° vs. $3 \times 109.5 = 328.5°$). The Al−N distances span a range from 2.009(5) (**1b**) to 2.038(9) Å (**1c**). This corresponds with the upper range of known Al−N distances in amine adducts of aluminum halides or hydrides, such as $AlCl_3$ · NMe_3 [d(Al−N) = 1.96(1) Å][15] or tmpH · AlH_3 [d(Al−N) = 2.04(1) Å][10]. Since chlorine and bromine have a stronger negative inductive effect than hydrogen, and thus increase the acceptor strength of the aluminum center, the Al−N distances in **1a**, **b** and **2** are shorter than that found

Table 1. Bonding parameters of compounds tmpH · AlX_3 (X = Cl, Br, I) and tmpH · AlH_2Cl

Parameter	tmpH·$AlCl_3$	tmpH·$AlBr_3$	tmpH·AlI_3	tmpH·AlH_2Cl
Bond lengths [Å]				
Al−N	2.014(2)	2.009(5)	2.038(9)	2.019(3)
Al−X(1)	2.129(1)	2.280(2)	2.540(3)	2.154(2)
Al−X(2); H(1)	2.136(1)	2.283(2)	2.535(3)	1.60(3)
Al−X(3); H(2)	2.129(1)	2.300(2)	2.532(3)	1.51(3)
Bond angles [°]				
N−Al−X(1)	99.86(7)	100.9(1)	99.0(3)	101.2(1)
N−Al−X(2); H(1)	115.39(8)	116.0(2)	118.6(3)	112(1)
N−Al−X(3); H(2)	116.72(7)	117.9(2)	119.2(3)	
X(1)−Al−X(3); H(2)	110.03(5)	110.02(8)	110.1(1)	109(1)
X(1)−Al−X(2); H(1)	110.83(5)	110.56(7)	109.3(1)	115.2(8)
X(3); H(2)−Al−X(2); H(2)	104.09(5)	101.59(7)	100.6(1)	108(2)
C(1)−N−Al	115.8(2)	117.1(3)	117.6(6)	114.8(2)
C(5)−N−Al	117.7(2)	117.4(3)	116.4(7)	114.7(2)
C(1)−N−C(5)	116.6(2)	115.7(4)	116.3(8)	116.9(2)

Figure 3. Molecular structure of tmpH · $AlCl_3$ (**1a**) in the solid state; thermal ellipsoids are shown at a 25% probability level; structural parameters are compiled in Table 1

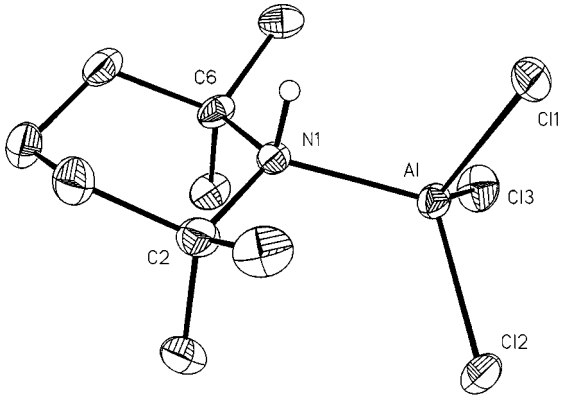

Figure 5. Molecular structure of tmpH · AlI_3 (**1c**) in the solid state; thermal ellipsoids are shown at a 25% probability level; structural parameters are compiled in Table 1

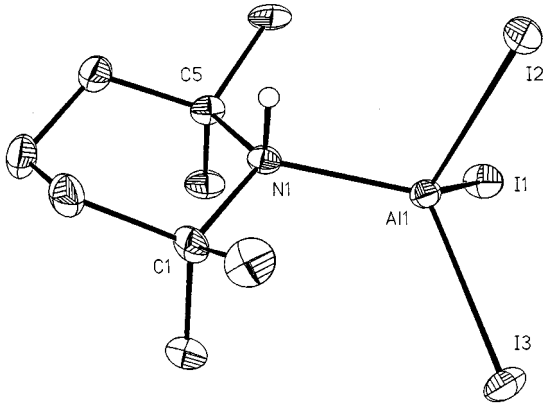

Figure 4. Stereoplot of the unit cell contents of tmpH · $AlBr_3$ (**1b**); view down the *c* axis (*a* axis to the right)

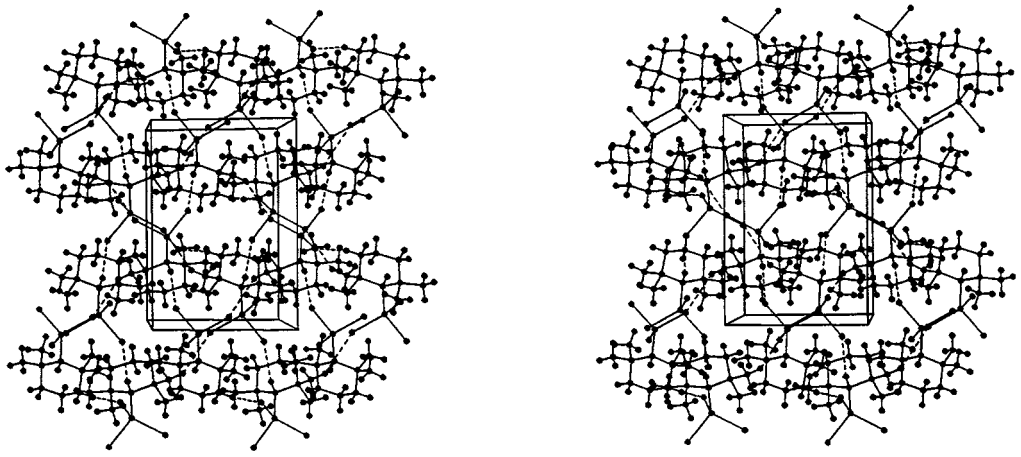

in tmpH · AlH_3. In **1c**, two opposing effects are responsible for the relatively long Al−N bond length: AlI_3 is the strongest Lewis acid amongst the aluminum halides[3], and, therefore, one would expect a short Al−N distance. However, the iodine atoms are considerably larger than the chlorine or bromine atoms and thus increase the steric strain. For this reason, *d*(Al−N) reaches its minimum values in **1a**, **b**, and not in **1c**. The aluminum−halogen bond lengths in these systems vary only slightly: the average Al−Cl distances are 2.131 Å (**1a**) and 2.154 Å (**2**), respectively, Al−Br is 2.288 Å (**1b**, av.), and Al−I is 2.536 Å (**1c**, av.). These values are close to those observed in $AlCl_3$ · NMe_3

Figure 6. Molecular structure of tmpH·AlH_2Cl (**2**) in the solid state; thermal ellipsoids are shown at a 25% probability level; structural parameters are compiled in Table 1

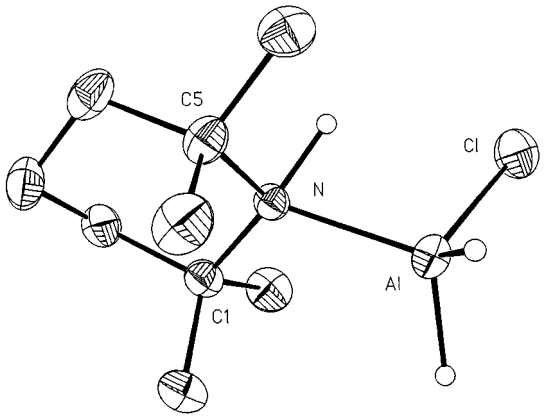

[d(Al−Cl) = 2.11(1)−2.14(1) Å][15], $AlMe_2I$ · NMe_3 [d(Al−I) = 2.58 Å][16] and AlI_3 · iq [iq = isoquinoline; d(Al−I) = 2.504(4) Å][13].

In spite of the fact that the adducts **1a−c** are present in space group No. 14, the arrangement of the molecules in the lattice is different in each case. Thus, in the chloride **1a**, the shortest intermolecular contacts are between a Cl atom of the $AlCl_3$ group and a hydrogen atom of a CH_3 group [(d(H···Cl) = 2.844 Å, angle Cl···H···C 169.7°]. In contrast, in **1b** there is an intermolecular N−H−Br contact with an H···Br distance of 2.978 Å (angle Br···H−N 169.0°) as well as an H···Br contact to a CH_3 group (3.019 Å). In the iodide **1c**, there are H···I contacts between two different I atoms and H atoms of two different CH_3 groups (4.021 and 3.191 Å, with Al−I···H angles of 148.2 and 125.7°, respectively). In contrast, there are no close intermolecular contacts between the Cl atom and H atoms bonded to either N or C in compound **2**.

Discussion

At first sight it is not easy to understand why only the aluminum trichloride adduct **1a** undergoes a structural change in solution. In fact, this could even be seen as a contradiction, because Atwood[11] found that only the bromo- and iodoalanes R_2AlX (X = Cl, Br, I; R = Me, Et) could be forced to ionize by the addition of excess tBuNH_2. This was attributed to the lower Al−Br and Al−I bond enthalpies and this argument should also be valid for the compounds described here. Since **1a** is found to "dissociate" according to Eq. 2, a decisive factor is clearly the formation of an ion pair (additional coulombic energy) and the chloro-bridged species tmpH · Al_2Cl_6. Thus, in this process nine terminal Al−Cl bonds are transformed into seven terminal and four bridging Al−Cl bonds. The relevant mean bond enthalpies are 425 kJ/mol for a terminal Al−Cl bond[3] and 289 kJ/mol for a bridging Al−Cl bond[17].

Table 2. Crystallographic data and information related to data collection and structure solution

Compound	tmpH · $AlCl_3$ (**1a**)	tmpH · $AlBr_3$ (**1b**)	tmpH · AlI_3 (**1c**)	AlH_2Cl · tmpH (**2**)
Chem. formula	$C_9H_{19}AlCl_3N$	$C_9H_{19}AlBr_3N$	$C_9H_{19}AlI_3N$	$C_9H_{21}AlClN$
Formula weight	238.12	407.96	548.93	205.71
Cryst. size [mm]	0.19 × 0.32 × 0.44	0.2 × 0.3 × 0.3	0.6 × 0.4 × 0.15	0.35 × 0.38 × 0.55
Crystal system	monoclinic	monoclinic	monoclinic	orthorhombic
Space group	$P2_1/n$	$P2_1/n$	$P2_1/c$	$P2_12_12_1$
a [Å]	8.682(2)	8.686(3)	16.126(4)	7.819(1)
b [Å]	12.233(2)	12.710(4)	13.628(4)	10.490(2)
c [A]	13.120(2)	13.339(5)	15.987(5)	15.224(3)
α [°]	90	90	90	90
β [°]	94.42(1)	96.47(1)	113.38(2)	90
γ [°]	90	90	90	90
V [Å^3]	1389.3(4)	1463.2(9)	3224.9(16)	1248.7(5)
Z	4	4	8	4
$\rho_{calcd.}$ [Mg/m^3]	1.138	1.852	2.261	1.094
μ [mm^{-1}]	0.495	8.300	5.843	0.334
absorption correction	−	semiempirical	semiempirical	−
min. and max. transmission	−	0.205 and 0.382	0.237 and 0.345	−
F(000)	504	792	2016	448
Index range	$-10 \le h \le 0$	$-9 \le h \le 9$	$-16 \le h \le 18$	$-13 \le h \le 0$
	$-14 \le k \le 0$	$-14 \le k \le 14$	$-15 \le k \le 0$	$-11 \le k \le 0$
	$-15 \le l \le 15$	$-14 \le l \le 14$	$-18 \le l \le 0$	$-12 \le l \le 22$
2θ [°]	50.00	46.52	48.10	50.00
T [K]	233	193	193(2)	293
Refl. collected	2619	6071	5304	3153
Refl. unique	2449	1937	5099	2192
Refl. obsd. (4σ)	1871	1666	4115	1827
R_{int}	0.0354	0.0413	0.0674	0.0276
No. of variables	127	131	261	118
Weighting scheme[a] x/y	0.1524/5.5644	0.0270/6.5814	0.0479/35.7622	0.0765/0.2610
GooF	0.649	1.102	1.176	0.1057
Final R (4σ)	0.0485	0.0392	0.0518	0.0443
Final $wR2$	0.1360	0.0854	0.1259	0.1209
Largest resid. peak [e/Å^3]	0.550	1.229	0.795	0.39

[a] $w^{-1} = \sigma^2F_o^2 + (xP)^2 + yP$; $P = (F_o^2 + 2F_c^2)/3$.

Hence, nine terminal Al−Cl bonds amount to an enthalpy of 3825 kJ/mol, while seven terminal and four bridging bonds represent 4131 kJ/mol, and consequently the "dissociated" species is favored by about 200 kJ/mol. As the bond enthalpies for Al−X−Al bridges decrease dramatically on going from X = Cl (ΔE_{bond} = 289 kJ/mol) to X = I (ΔE_{bond} = 192 kJ/mol)[17], the formation of halide bridges is not favored for X = Br, I. Due to the large steric requirement of the tetramethylpiperidine ligand, another usual pathway to dissociation, as described by Eq. 3, is not applicable here.

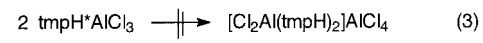

Figure 7. Calculated heats of formation of all compounds involved in Eq. 4 and estimated enthalpy of formation of tmpH · Al_2Cl_6 and [tmpAlCl$_3$]tmpH$_2$

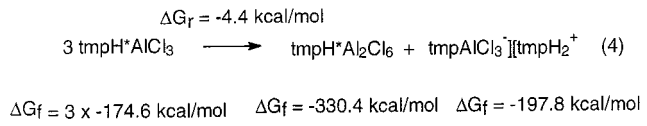

This assumption is corroborated by a semiempirical AM1 calculation[18] of all the heats of formation of compounds that appear in Eq. 4 (see Figure 7). This allows an estimate of the overall reaction enthalpy. In the gas phase, the dissociated species are found to be favored by about 4.4 kcal/mol over the molecular starting material. Moreover, polar solvents such as dichloromethane should exert an additional stabilizing effect, thereby assisting in the formation of ion pairs. As this additional stabilization is not provided by the crystal lattice, the undissociated monomeric species **1a** turns out to be more stable in the solid state.

Conclusion

The tetramethylpiperidine alane adducts **1a−c** and **2** are stable towards HX and H_2 elimination, and thus formation of compounds tmpAlX$_2$ or tmpAl(H)X does not occur. In the solid state, they are present as monomeric tetracoordinated species. This is also true for solutions of **1b**, **c** and **2**. In contrast, upon dissolution of tmpH · $AlCl_3$, a transformation takes place according to Eq. 2. Whether this behavior is general or is specific to this compound will be addressed in future investigations; it is surprising to us that such simple systems raise such interesting and unforeseen questions.

We thank the *Fonds der Chemischen Industrie* and the *Chemetall mbH* for support of our research. We are also grateful to Mrs. *Käser* and Mrs. *R. Ullmann* for performing C/H/N analyses, Mr. *P. Mayr*, Dr. *R. Waldhör* and Dr. *C. Miller* for recording many NMR spectra, Mrs. *D. Ewald* for mass spectra and Mrs. *E. Kiesewetter* for IR spectra.

Experimental Section

All manipulations were performed using Schlenk techniques under dinitrogen. All solvents were rigorously dried prior to use and stored under dinitrogen or argon. − NMR: Bruker ACP 200, Jeol GSX400, and Jeol GSX270. − IR: Nicolet FT-IR spectrometer model 6000, CsI plates, Nujol. − MS: Varian Atlas CH7 spectrometer.

tmpH · $AlCl_3$ (**1a**): To a suspension of $AlCl_3$ (0.65 g, 4.87 mmol) in 10 ml of CH_2Cl_2, tmpH (0.83 ml, 4.87 mmol) was added at ambient temperature and the mixture was exposed to ultrasound for 3 h. The resulting yellow solution was stored at −20°C overnight, whereupon 0.90 g (67%) of colorless crystals of tmpH · $AlCl_3$ separated, m.p. 130°C. − ^{1}H NMR ($CDCl_3$, 400 MHz): δ = 1.40 (s, 12 H, tmp-CH_3), 1.61 (s, 12 H, tmp-CH_3), 1.73 (s, 12 H, tmp-CH_3), 2.88 (br. s, 2 H, N-*H*), 4.83 (br. s, 1 H, N-*H*), some additional multiplets at δ = 1.45 and 1.60−1.80 were also observed, but were not readily assigned. − ^{13}C NMR ($CDCl_3$, 100 MHz): δ = 15.7 (tmp-γ-*C*H$_2$), 16.5 (tmp-γ-*C*H$_2$), 23.5 (tmp-*C*H$_3$), 29.1 (tmp-*C*H$_3$), 33.5 (tmp-*C*H$_3$), 36.1 (tmp-*C*), 41.1 (tmp-*C*), 53.3 (tmp-*C*), 57.2 (tmp-*C*), 59.6 (tmp-*C*). − ^{27}Al NMR ($CDCl_3$, 70 MHz): δ = 106 ($\Delta_{1/2}$ = 47 Hz), 108 ($\Delta_{1/2}$ = 120 Hz). − IR (Nujol): $\tilde{\nu}$ = 3172 cm^{-1} s (N−H), 496 ss (Al−Cl), 421 ss (Al−Cl). − $C_9H_{19}NAlCl_3$ (274.60): calcd. C 39.37, H 6.97, N 5.10; found C 38.33, H 7.02, N 4.97.

tmpH · $AlBr_3$ (**1b**): tmpH (0.85 ml, 5.0 mmol) in 5 ml of benzene was added to a solution of $AlBr_3$ (1.3 g, 5.0 mmol) in 20 ml of benzene with stirring. The addition was accompanied by an immediate color change from brown to light-yellow. Successive partial evaporation of the solvent and cooling to 8°C led to the precipitation of colorless crystals of tmpH · $AlBr_3$. These were recrystallized from 15 ml of benzene, m.p. 137−139°C (darkening). Yield of **1b**: 1.46 g (76%). − ^{1}H NMR (C_6D_6, 270 MHz): δ = 0.35 (m, 1 H, tmp-CH_2), 0.52 (m, 1 H, tmp-CH_2), 0.72 (dt, 2 H, tmp-CH_2), 0.91 (dt, 2 H, tmp-CH_2), 1.20 (s, 6 H, tmp-CH_3), 1.53 (s 6 H, tmp-CH_3). − ^{13}C NMR (C_6D_6, 100 MHz): δ = 15.3 (tmp-*C*4), 23.6, 33.8 (tmp-*C*7-10), 40.8 (tmp-*C*3,5), 60.1 (tmp-*C*-N). − ^{27}Al NMR (C_6D_6, 70 MHz): δ = 88 ($\Delta_{1/2}$ = 130 Hz). − IR (Nujol) [ν(Al−Br) range]: $\tilde{\nu}$ = 411 cm^{-1} vs, 384 s. − $C_9H_{19}NAlBr_3$ (407.95): calcd. C 26.50, H 4.69, N 3.43, Al 6.6, Br 58.8; found C 27.18, H 5.13, N 3.17, Al 6.7, Br 60.4.

tmpH · AlI_3 (**1c**): To a solution of AlI_3 (0.81 g, 2.0 mmol) in 20 ml of toluene, a solution of tmpH (0.34 ml, 2.0 mmol) in 5 ml of toluene was added at ambient temperature. The addition was accompanied by an immediate color change from brown to yellow. The resulting solution was reduced to one-third of its original volume. Upon cooling to −20°C, colorless crystals of tmpH · AlI_3 separated, which were recrystallized from 10 ml of toluene; m.p. 141−143°C (decomp.), yield of **1c**: 0.81 g (74%). − ^{1}H NMR (C_6D_6, 270 MHz): δ = 0.33 (m, 1 H, tmp-CH_2), 0.56 (m, 1 H, tmp-CH_2), 0.81 (dt, 2 H, tmp-CH_2), 1.00 (dt, 2 H, tmp-CH_2), 1.25 (s, 6 H, tmp-CH_3), 1.70 (s, 6 H, tmp-CH_3). − ^{13}C NMR (C_6D_6, 100 MHz): δ = 14.4 (tmp-*C*4), 23.5, 33.9 (tmp-*C*7-10), 41.1 (tmp-*C*3,5), 60.4 (tmp-*C*-N). − ^{27}Al NMR (C_6D_6, 70 MHz): δ = 12 ($\Delta_{1/2}$ = 140 Hz). − IR (Nujol) [ν(Al−I) range]: $\tilde{\nu}$ = 347 cm^{-1} vs, 295 s. − $C_9H_{19}NAlI_3$ (548.95): calcd. C 19.69, H 3.49, N 2.55, Al 4.9, I 69.4; found C 19.66, H 3.72, N 2.50, Al 5.3, I 70.1.

tmpH · AlH_2Cl (**2**): To a solution of $AlH_2Cl(thf)_2$ (14.1 g, 67.4 mmol) in 50 ml of thf, 11.5 ml of tmpH (67.4 mmol) in 50 ml of toluene was added at −40°C. The mixture was allowed to warm to ambient temperature and was then heated to reflux for 3 h. Thereafter, all volatiles were removed in vacuo and the residue was extracted with 100 ml of pentane. The organic extract was filtered to afford a colorless solution. Cooling to −20°C provided 10.1 g (72%) of colorless crystals of **2**, m.p. 85°C. − ^{1}H NMR (C_6D_6, 270 MHz): δ = 0.84 (m, 4 H, tmp-β-CH_2), 1.16 (s, 12 H, tmp-CH_3), 1.68 (s, 2 H, tmp-γ-CH_2). − ^{13}C NMR (C_6D_6, 100 MHz): δ = 18.8

(tmp-*C*4), 32.4 (tmp-*C*7-10), 38.6 (tmp-*C*3,5), 49.6 (tmp-*C*-N). – ^{27}Al NMR (C_6D_6, 70 MHz): δ = 123. – IR (Nujol): $\tilde{\nu}$ = 1891 cm^{-1} vs, 1831 vs [ν(AlH)], [ν(N–H) range] 3137 m [ν(NH)]. – $C_9H_{21}NAlH_2Cl$ (205.7): calcd. Al 13.1, Cl 17.3; found Al 12.3, Cl 18.6.

X-ray Crystal-Structure Determinations: Data collection for X-ray structure determinations was performed with a Siemens P4 or a Syntex R3 four-circle diffractometer using graphite-monochromated Mo-K_α (λ = 0.71073 Å) radiation. Single crystals were mounted in Lindemann capillaries and sealed under argon. Data collection was performed at −80 to −100°C. All calculations were performed with PCs and workstations using the Siemens SHELXTL-Plus[19] or SHELX-93[20] software packages. The structures were solved by direct or heavy-atom methods with successive interpretation of the difference Fourier maps, followed by least-squares refinement. All non-hydrogen atoms were refined anisotropically. The hydrogen atoms were included in the refinement in calculated positions by a riding model using fixed isotropic parameters. Data relevant to the crystallography, data collection and refinement are compiled in Table 2. Further details on the crystal structure determinations have been deposited at the Cambridge Crystallographic Data Centre and may be requested by quoting the depository number CSD-103180 (**1a**), -103181 (**1b**), -103182 (**1c**) and -103183 (**2**), the names of the authors, and the full journal citation.

☆ Dedicated to Prof. Dr. *M. Weidenbruch* on the occasion of his 60th birthday.

[1] I. Krossing, Ph. D. Thesis, University of Munich, **1997**.
[2] X-ray crystal structures.
[3] A. J. Downs (Ed.), *Chemistry of Aluminium, Gallium, Indium, and Thallium*, Blackie Academic and Professional, London, **1993**, p. 430.
[4] P. J. Olgren, J. P. Cannon, C. F. Smith, Jr., *J. Phys. Chem.* **1971**, *75*, 282–289.
[5] L. Jakobsmeier, I. Krossing, H. Nöth, M. J. H. Schmidt, *Z. Anorg. Allg. Chem.* **1996**, *51b*, 1117–1126.
[6] [6a] P. Pullmann, K. Hensen, J. W. Bats, *Z. Naturforsch., Part B* **1982**, *37*, 1312–1316. – [6b] D. M. Brown, D. T. Stewart, D. E. H. Jones, *Spectrochim. Acta* **1973**, *29a*, 213–217. – [6c] M. Dalibart, J. Derouault, M. T. Forel, *J. Mol. Struct.* **1981**, *70*, 119–123.
[7] J. Meunier, M. T. Forel, *Can. J. Chem.* **1972**, *50*, 1157–1161.
[8] I. R. Beattie, P. J. Jones, J. A. K. Howard, L. E. Smart, C. J. Gilmore, J. W. Akitt, *J. Chem. Soc., Dalton Trans.* **1979**, 528–541.
[9] H. Nöth, R. Rurländer, P. Wolfgardt, *Z. Naturforsch., Part B* **1982**, *37*, 29–35.
[10] J. L. Atwood, G. A. Koutsantonis, F. C. Lee, C. L. Raston, *J. Chem. Soc., Chem. Commun.* **1994**, 91–92.
[11] D. A. Atwood, J. Jegler, *Inorg. Chem.* **1996**, *35*, 4277–4282.
[12] [12a] I. Krossing, H. Nöth, C. Tacke, M. Schmidt, H. Schwenk, *Chem. Ber.* **1997**, *130*, 1047–1052. – [12b] I. Krossing, H. Nöth, B. N. Anand, *Inorg. Chem.* **1997**, *36*, 1979–1981. – [12c] K. Knabel, I. Krossing, H. Nöth, M. Schmidt-Amelunxen, H. Schwenk-Kircher, *Eur. J. Inorg. Chem.*, to be submitted.
[13] I. Krossing, H. Nöth, H. Schwenk-Kircher, *Eur. J. Inorg. Chem.*, to be submitted.
[14] R. M. Fuoss, C. A. Kraus, *J. Am. Chem. Soc.* **1933**, *55*, 2387–2399.
[15] A. Haaland, *Angew. Chem.* **1989**, *101*, 1017–1032; *Angew. Chem. Int. Ed. Engl.* **1989**, *28*, 992.
[16] J. L. Atwood, P. A. Milton, *J. Organomet. Chem.* **1973**, *52*, 275–279.
[17] K. Wade, A. J. Banister, *The Chemistry of Aluminum, Gallium, Indium and Thallium*, Pergamon Press, Oxford, **1975**.
[18] Performed with the program *Hyperchem*, V3.0, Autodesk, **1993**.
[19] *PC SHELXTL Rel. 5.03*, Siemens Analytical Instruments, Version 4.1, **1994**.
[20] G. M. Sheldrick, University of Göttingen, **1993**.

[97286]